Carbon nanotubes for gas detection: materials preparation and device assembly

2007 J. Phys.: Condens. Matter 19 225004

(http://iopscience.iop.org/0953-8984/19/22/225004)

IOP PUBLISHING JOURNAL OF PHYSICS: CONDENSED MATTER

J. Phys.: Condens. Matter **19** (2007) 225004 (14pp) doi:10.1088/0953-8984/19/22/225004

Carbon nanotubes for gas detection: materials preparation and device assembly

M L Terranova[1,2,4], M Lucci[1,2,3], S Orlanducci[1,2], E Tamburri[1,2], V Sessa[1,2], A Reale[2,3] and A Di Carlo[2,3]

[1] Dipartimento di Scienze e Tecnologie Chimiche, Università di Roma 'Tor Vergata'—Via della Ricerca Scientifica, 00133 Roma, Italy
[2] Interdisciplinary MIcro and NAno-structured Systems Laboratory (MINAS), Università Roma Tor Vergata, Italy
[3] Dipartimento di Ingegneria Elettronica, Università di Roma 'Tor Vergata'—Via del Politecnico 1, 00133 Roma, Italy

E-mail: marialetizia.terranova@roma2.infn.it

Received 25 July 2006, in final form 26 September 2006
Published 14 May 2007
Online at stacks.iop.org/JPhysCM/19/225004

Abstract

An efficient sensing device for NH_3 and NO_x detection has been realized using ordered arrays of single-walled C nanotubes deposited onto an interdigitated electrode platform operating at room temperature. The sensing material has been prepared using several chemical–physical techniques for purification and positioning of the nanotubes inside the electrode gaps. In particular, both DC and AC fields have been applied in order to move and to align the nanostructures by electrophoresis and dielectrophoresis processes. We investigated the effects of different voltages applied to a gate contact on the back side of the substrate on the performances of the device and found that for different gas species (NH_3, NO_x) a constant gate bias increases the sensitivity for gas detection. Moreover, in this paper we demonstrate that a pulsed bias applied to the gate contact facilitates the gas interaction with the nanotubes, either reducing the absorption times or accelerating the desorption times, thus providing a fast acceleration and a dramatic improvement of the time dependent behaviour of the device.

1. Introduction

Single-walled carbon nanotubes (SWNTs) are nowadays one of the most investigated materials, and the realization of ordered SWNT structures is of fundamental importance for the improvement of many technological fields, from non-linear optics [1] to the realization of transistors [2] to the assembly of gas sensing devices [3].

[4] Author to whom any correspondence should be addressed.

0953-8984/07/225004+14$30.00

An SWNT is formed by rolling a graphene sheet into a seamless cylinder with a diameter on the nanometre scale [4]. The individual SWNTs are joined to each other and assembled into bundles by van der Waals forces. Guest molecules can potentially interact with SWNTs via the outer surfaces of bundles, the inside of the tubes and/or the interstitial channels between the tubes in a bundle. These different situations are expected to play an important role in tuning the guest molecule/SWNT interaction during gas adsorption and/or desorption, and have been investigated theoretically [5] and experimentally [6] using different approaches.

In particular, the interaction between gaseous molecules and SWNTs has been investigated from different points of view, including gas storage [7, 8] and gas detection through modification of electronic and thermal properties [6, 9–14] or through modification of the field emission properties [15, 16]. Compared with conventional solid-state sensors, that typically operate at temperatures over 400 °C, and conducting polymer-based sensors, that provide only limited sensitivity, sensing devices assembled with single-wall nanotubes can exhibit high sensitivity and fast response time at room temperature [13, 14].

Due to the high surface area of nanotubes, a small amount of nanotube material can provide many sites for gas interaction [17, 18]. The accessibility of these sites depends on the status of aggregation of the nanotubes. Our preliminary studies [3] suggested that the sensitivity of a nanotube-based device can be optimized by controlling the organization of the SWNTs. Ordered bundles of SWNTs indeed exhibit a sensitivity double that of a disordered deposit. This is probably due to the enhancement of surface area for organized SWNT systems with respect to randomly placed SWNT bundles.

Hence, aligned nanotubes can serve as a very efficient material for use in gas detection. Directionality of the SWNTs can be obtained directly during the synthesis process [19], or after manipulation of dispersed nanotubes, by means of several methods, such as filtration/deposition from suspension in strong magnetic fields [20], field emission [21], electrophoresis or dielectrophoretic processes. In particular, the use of electric fields to move, position and align SWNTs has been reported in recent papers [22–28], and the results indicate that both the electrophoresis (EP) and dielectrophoresis (DEP) routes have potential advantages for arranging nanotubes in controlled systems.

Beyond the sensitivity, another severe constraint for gas detection is the time either for the reset of the sensor after exposure to the gas, or for the acceleration of the response itself.

Since practical applications can be severely limited by slow absorption/desorption processes, we felt it worthwhile to investigate in a systematic way some physical parameters affecting the sensor response.

In this paper we present a study of NH_3 and NO_x detection using organized SWNTs as sensing material and an innovative procedure to improve the time response of the sensor by applying a back-gate voltage.

2. Experimental details

2.1. Materials preparation

Samples of Carbolex SWNTs (purity 50–70%) used in these experiments were purified following two different procedures, both based on the oxidation by HNO_3. The first one, which has been used for the samples named 'A', makes use of 2 M HNO_3 at 25 °C [29]. This treatment is able to eliminate the catalyst particles and to eliminate partially the spurious carbonaceous species. The advantage of this mild treatment is that the SWNTs are not structurally modified or functionalized. Following the second procedure, the samples (hereinafter called samples B) are treated in HNO_3 2 M at 100 °C for 1 h. This purification process helps in eliminating a larger number of carbon impurities, but can induce defects on the structure of the final

material. Raman spectroscopy and reflection high-energy electron diffraction (RHEED) have been routinely used to check structural features and phase purity of the material before purification and at the various stages of the chemical–physical treatments.

We checked moreover the feasibility of moving the SWNTs and of separating them from residual impurity particles by means of field-generated forces. A series of experiments have been carried out by applying AC and DC electric fields to SWNTs containing dispersions.

However, the process of migration of nanotubes and debris under an electric field is found to depend not only on the characteristics of the field itself, but also on the properties of the SWNTs and of their suspensions. In particular, the chemical state of the SWNTs, the volatility and the dielectric properties of the solvents turn out to be critical parameters.

In order to investigate the effect of different mobility times on the field-induced alignment of nanotube-based systems, we tested some diluents commonly used to prepare carbon nanotube dispersions, such as chloroform ($CHCl_3$), acetone (CH_3COCH_3), acetonitrile (CH_3CN) and dimethylformamide (DMF) ($HCON(CH_3)_2$). These diluents are characterized by different dielectric properties but also by very different evaporation times. For example, the times for complete evaporation of 35 μl of chloroform and DMF are, at room temperature, 120 s and 240 min, respectively.

To prepare the suspensions, 3 mg of the treated nanotube samples were dispersed in 250 ml of DMF, CH_3CN, CH_3COCH_3 or $CHCl_3$. Controlled aliquots (35 μl) of the suspensions were micro-pipetted to fill the gaps between the Cr–Au coplanar interdigitated electrodes of a multifinger sensing device. The Cr/Au electrodes (40 μm spacing) were patterned over a SiO_2 insulating layer deposited onto the p-doped silicon substrate. An image of the sensor can be found in [3].

The controlled placement of SWNTs was assisted by alternating (AC) or constant (DC) electric fields obtained through the application at the electrodes of different potentials. For AC experiments we applied sinusoidal potentials in the range 6–10 V_{pp} with frequencies ranging between 100 kHz and 10 MHz, for DC experiments a 6 V constant bias.

The electric fields produced by the computer controlled power supplies were applied to the multifingers until complete evaporation of the solvent. At the end of the process the morphology of the materials deposited onto the interdigitated electrodes was investigated by a field emission scanning electron microscope (FE-SEM) and the I–V characteristics were measured at room temperature and under vacuum ($P = 10^{-2}$ mbar) by using a 4155B Agilent semiconductor parameter analyser.

We tested in a systematic way SWNT samples obtained using both treatments and dispersed in the various solvents.

In the absence of applied field, independently from the nanotube treatment and from the medium, a random placement of SWNTs on the interdigitated electrodes was obtained.

Conversely, the AC and DC fields are found to affect specifically the alignment of the nanotube bundles and their separation from charged impurities.

In the case of DC electric field, electrophoretic forces act driving all the charged species, which include both impurity particles and nanotubes. Some of these species turn out to be negatively charged because of the presence, at their surface, of NO^{3-} ions adsorbed during the purification treatments. The DC field can be used to separate nanotubes from particles because the charged impurities with spherical or quasi-spherical shape are subjected to stronger electrophoretic forces and are preferentially drifted toward the positive electrode (figure 1(a)).

This effect is evident when using diluents with short evaporation times, such as $CHCl_3$. In figure 1(a) it is possible to appreciate the situation for an A-type sample dispersed in $CHCl_3$. After the EP process the particles are very close to the positive electrode, while they are completely swept away from the negative electrode (figure 1(b)).

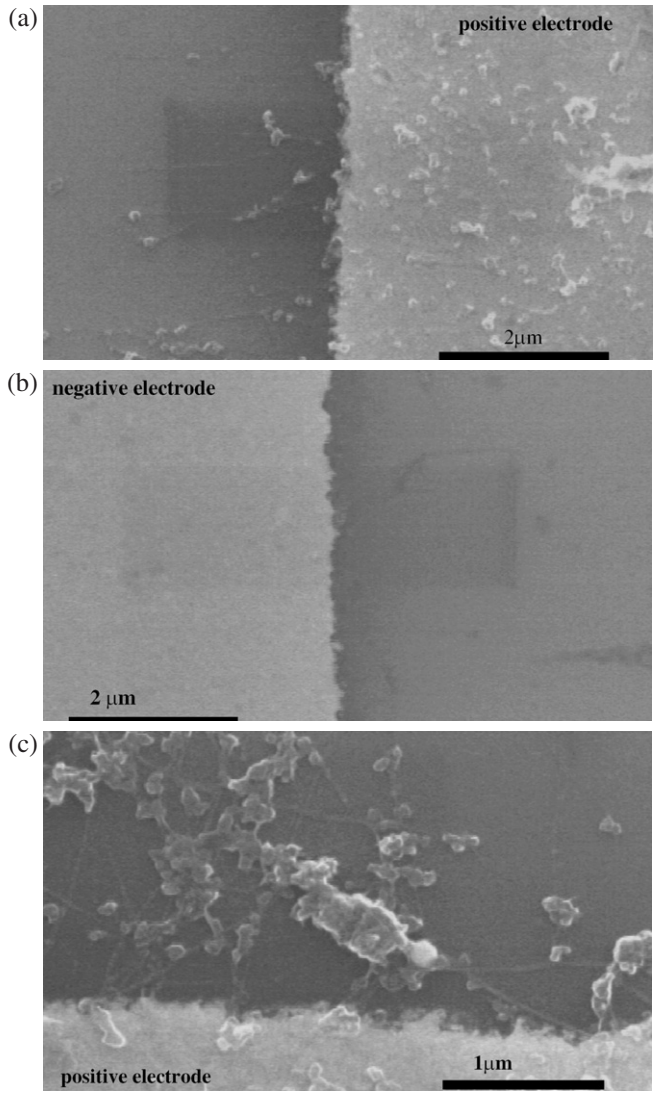

Figure 1. FE-SEM images of electrodes at the end of EP processes (6 V DC field): (a) positive electrode, $CHCl_3$ dispersion; (b) negative electrode, $CHCl_3$ dispersion; (c) positive electrode, DMF dispersion. The nanotubes were of the 'A' type.

However, in the case of DMF, thanks to the evaporation time of about 2 h, the electrophoretic process is also effective for the drifting of the SWNT bundles that are driven toward the positive electrode, together with the impurities (figure 1(c)). The morphological analysis shows that there is no order in the bundles drifted at the positive electrode.

A different situation is produced when applying AC fields. Under the action of AC fields the polarization induced in the medium and in SWNTs creates a dielectrophoretic force which moves and tends to align the ropes along the electric field lines, perpendicularly to the electrode stripes.

The DEP force is also able to extract, move and align bundles protruding from complex structures and densely packed aggregates. This effect is observed independently from the

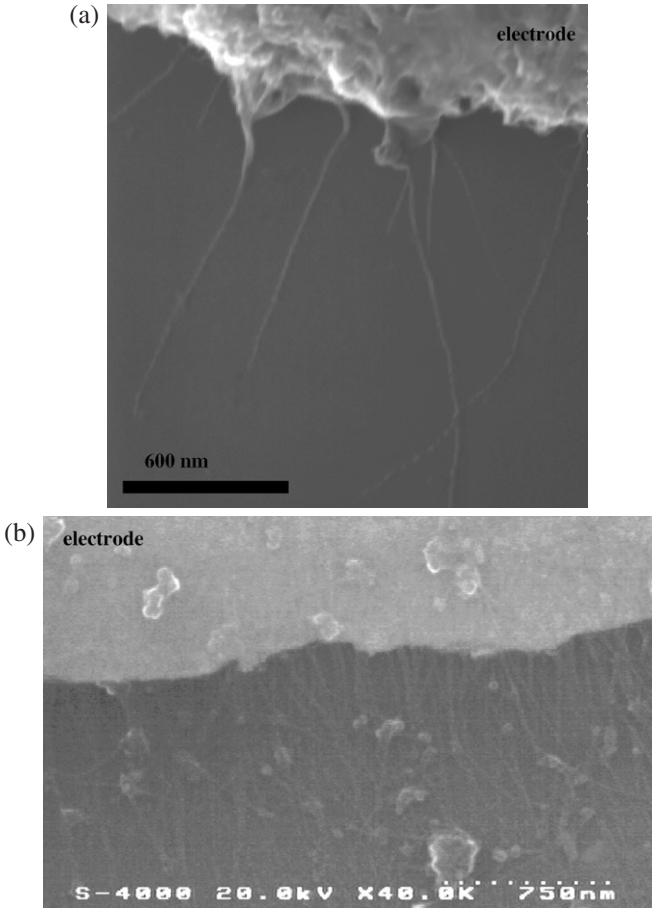

Figure 2. FE-SEM images of SWNT bundles at the positive electrode after the DEP process (10 V_{pp}, 1 MHz AC field): (a) $CHCl_3$ dispersion; (b) DMF dispersion.

solvent used for the nanotube dispersion. Figure 2(a) shows SWNT bundles well aligned and rather orthogonally placed at the positive electrode after a process induced in a SWNT/$CHCl_3$ dispersion by an AC field (10 V_{pp}, frequency 1 MHz). In the case of solvents with lower volatility the efficiency of the dielectrophoretic process is strongly enhanced. For an SWNT/DMF dispersion, the long exposure to the same AC field allows us to move the nanotubes but also the debris toward the positive electrode, as shown in figure 2(b).

A comparison of the conductive behaviour of different nanotube deposits is reported in figure 3. The I/V curves of figure 3(a) refer to SWNT/$CHCl_3$ dispersions, those of figure 3(b) to SWNT/DMF dispersions. Both the dispersions were prepared using nanotubes purified following the same procedure.

For both the $CHCl_3$ and the DMF solvents the samples obtained by using the AC fields present a higher conductibility with respect to the case of DC field.

The lower conductivity values detected for samples obtained by electrophoresis is probably due to the fact that under DC field both charged particles and SWNTs were found to move toward the positive electrode and no bridges were created between the electrodes. As expected, the conductivity decrease is more evident using DMF (figure 3(b)).

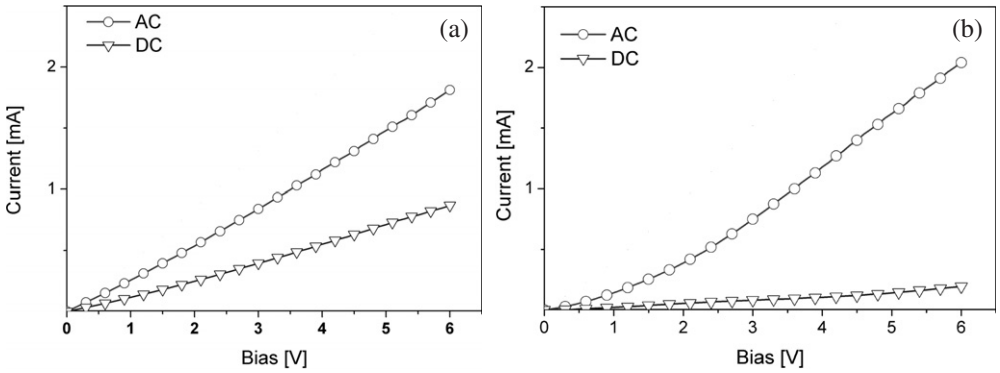

Figure 3. *I–V* measurements of SWNT bundles deposited under AC (10 V_{pp}, 1 MHz) and DC (6 V_{pp}) electric field: (a) $CHCl_3$ dispersion; (b) DMF dispersion.

The frequency analysis was done using 10 V_{pp} voltages at 100 kHz, 1 MHz, 5 MHz and 10 MHz respectively, and $CHCl_3$ as solvent.

Also in this case we tested both the A and B SWNT samples. Of particular interest was the frequency analysis performed on the A samples, reported in the following.

The FE-SEM investigations indicated that the SWNTs begin to experience the DEP force at 100 kHz. At 1 MHz an increase of the SWNT alignment and the beginning of the migration of impurity particles towards the fingers were observed. At 5 MHz the debris is furthermore driven towards the electrodes, whereas the alignment of SWNTs is less evident.

At 10 MHz the onset of an interesting behaviour is observed. The application of the electric field indeed produces effects opposite to those detected in all the previous cases. In this case both the SWNT bundles and impurity particles are swept far away from the electrodes, and collected in the gap between the interdigitated fingers. This seems to indicate the occurrence, at frequencies around 10 MHz, of a transition from positive to negative DEP forces.

These results indicate the possibility of using DEP at selected frequencies as an alternative method for the purification of nanostructures.

The trend of conductivity versus frequency, shown in figure 4, is in good agreement with the above reported observations. In the range 100 kHz–5 MHz a slight decrease of the conductivity is indeed observed. At 10 MHz the conductivity drops because no SWNTs or particles are participating in the conduction mechanism between the electrodes.

For the sensor assembly we used SWNTs purified using the second procedure (samples B) and dispersed in $CHCl_3$. The deposition of the material onto the multifinger device was accomplished under AC field (10 V_{pp}, 1 MHz). Our investigations indicated that under these conditions a better compromise between alignment of nanotubes and conductivity could be obtained.

2.2. Device assembly

The interdigitated electrode platform was placed in a gas chamber connected with a fluxmeter and used as the gas sensing element.

Gate control and heating control of the device are obtained positioning the back side of the Si element on a metal holder contacting the element face.

The state of the sensor (gate voltage, heating) is controlled by a computer interface for data acquisition and signal management.

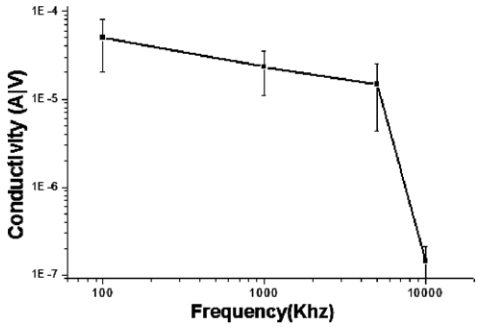

Figure 4. Conductivity of the SWNT bundles deposited under AC field (10 V_{pp}) at 100 kHz, 1 MHz, 5 MHz and 10 MHz.

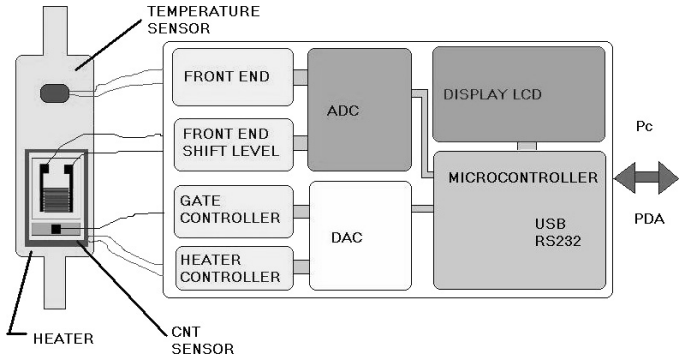

Figure 5. A scheme of the gas sensing experimental set-up.

The resistance of the sensor is read by a front-end block and transduced in an electrical signal in the range 0–5 V. The resistance and temperature values are converted by an ADC block into numeric values (10–24 bit), which are in turn read by a micro-controller, mathematically elaborated and finally transmitted using an opportune communication protocol. The bi-directional communication from the micro-controller to another terminal occurs through a USB or an RS232 port. Typical terminal devices to be connected with the micro-controller are PC, PDA or video terminals.

Commands from PC or PDA to the micro-controller produce the appropriate voltages for the gate pin. The signals coming from the micro-controller are converted into 0–5 V signals by a DAC block and by a controller as proper signals to drive the gate. Gate bias was in the range −40 V, +40 V.

A scheme of the experimental set-up is reported in figure 5.

This system is able to read the signals coming from many elements (up to 13) and therefore it is possible to realize sensing devices formed by arrays of different sensors, where the information can be obtained by a mathematical analysis of the data.

In order to check the detecting performances of the device we selected two chemical species, namely NO_x and NH_3, representative of electron-acceptor and electron-donor systems.

For NO_x detection, different concentrations in the range 0.1–10 ppm have been produced by diluting the gas in N_2.

In the case of NH_3, a solution of NH_3 in H_2O (concentration: 30 vol.%) was put in a bubbler in parallel with a N_2 flux. A series of gaseous NH_3/N_2 mixtures, with NH_3 ranging between 5 and 750 ppm, was obtained controlling the gas flow. To exclude the effect of water the sensor was also tested using a standard NH_3 gas bottle.

3. Results and discussion

Previous experiments indicated the feasibility of nanotube-based sensors to detect at room temperature ppm or sub-ppm amounts of NH_3 and NO_x. Moreover, linear trends of response (expressed as $(\Delta R/R)$/ppm) increasing with increase of concentration were found for both NH_3 and NO_x and improvements of the sensitivity were evidenced when using aligned bundles of nanotubes [30]. As evidenced from experiments some gases, when adsorbed, are able to modify the electrical properties of SWCNT ensembles, because they change the density of states at the Fermi level of semiconducting nanotubes.

The induced effects, in particular the change in conductivity, depend on both the electronic structure of the gaseous species and on their adsorption mechanism.

Theoretical studies [31] indicated that NH_3 gas molecules are weakly bonded to nanotubes and that the tube–molecule interaction can be identified as a physisorption. Moreover, NH_3 has an electron-donor behaviour with a small charge transfer (0.031 e per molecule) and weak binding energy (0.2 eV). Instead, NO_x has an electron acceptor behaviour with significative charge transfer (-0.07 e per molecule) and higher binding energy (0.7 eV). This difference is also confirmed from our experiment, where the sensitivity to NO_x is higher than NH_3.

From the experimental data it is possible to deduce a p-type behaviour for our CNT's sensor. Figure 6 shows the resistance changes detected upon exposure of the interdigitated electrode platform, for a fixed time of 15 min, to 100 ppm of NH_3 (figure 6(a)) and 650 ppb NO_x (figure 6(b)) respectively. As is seen, the electron donor NH_3 acts by increasing the resistivity of the nanotubes, the electron acceptor NO_x by decreasing the resistivity.

The CNT's sensor shows a response G to the gas similar to semiconducting oxide gas-sensitive resistors, that is empirically represented as follows [32]:

$$G = A_g P_g^{\beta} \tag{1}$$

where P_g is the target gas partial pressure. The term G is expressed by $(R - R_0)/R_0$ for resistance (R) increase, or by $(\sigma - \sigma_0)/\sigma_0$ for resistance decrease (σ is the conductance). R_0 and σ_0 are the values of resistance and conductance, respectively, in the absence of the gas under investigation. The response is characterized by the sensitivity, A_g, and by an exponent, β. For the surface reactions, mechanisms may be formulated which predict the form of equation (1) with β in the range 0.5–1 [32].

The linear trend of the response in the low range of concentration is due to the high number of interaction sites typical of our sensor and to the low surface coverage in our working regime.

However, these experiments show a not instantaneous response of the sensor. As evidenced in figure 6(a), after exposure to 100 ppm of NH_3 the base line of resistance is approached in approximately 100 min from the gas inlet. This is due to the high surface area of the CNTs, i.e. high number of interaction sites, thus high probability to interact with gas. This allows us to obtain a high sensitivity, but needs a long time to obtain an equilibrium between gas and sensible species (CNTs) evidenced by a stable value of resistivity. Also desorption times, that represent a fundamental characteristic of gas sensors, were found to be exceedingly long. As an example, the complete desorption of NH_3 was achieved in approximately 150 min.

Significative changes in the device response have been conversely obtained applying a voltage between the back-gate contact and one of the electrodes.

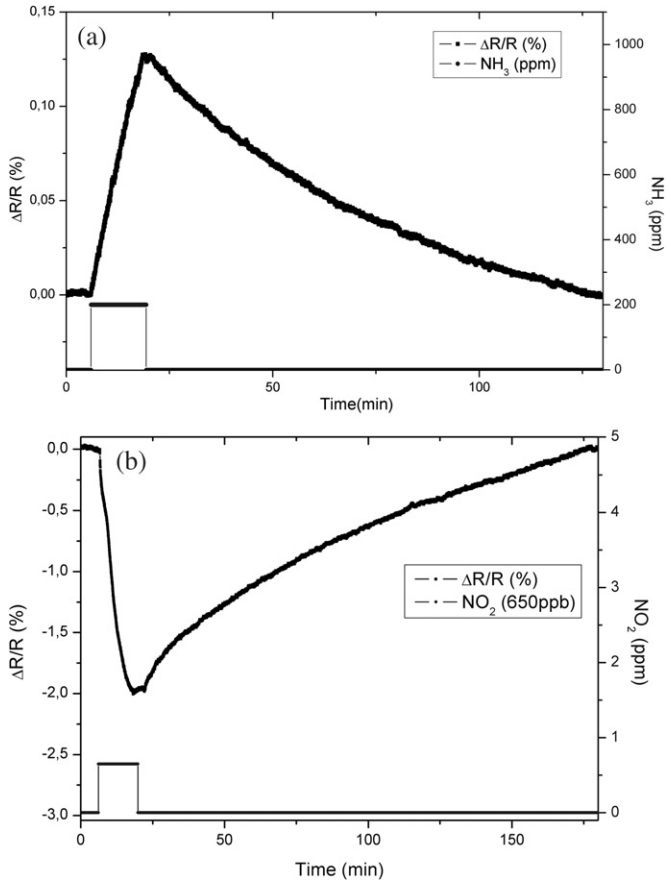

Figure 6. Resistance changes detected by the sensor upon gas exposure for a fixed time of 15 min: (a) NH_3 (100 ppm); (b) NO_x (650 ppb).

The resistance changes induced in the SWNTs at back-gate constant voltages of -20, 0 and $+20$ V, respectively, have been measured for NH_3 under stationary conditions. From these data the relative sensitivities of the sensor, $(\Delta R/R)$/ppm, have been calculated. As expected, the sensor exhibits a quite different behaviour depending on the bias [33, 34]. For the same NH_3 concentration (150 ppm), the conductance was found to vary in the range $+10\%$ to -10% The values of relative sensitivity were 0.374%/ppm in the absence of voltage, 0.428%/ppm for -20 V, and 0.239%/ppm for $+20$ V. No saturation regime of the I–V curves was observed up to $+20$ V, a limiting voltage value to prevent destruction of the multifinger interdigitates themselves.

The effect of biasing the back-gate contact deserves even more attention. As a matter of fact we have found that the gate voltages affect dramatically not only the overall sensitivity but also the response time of the device.

The effects produced by the positive and negative biasing pulses on the response times for NH_3 detection are presented in figure 7. Figure 7(a) illustrates how the negative voltage pulse on the gate reduces the absorption time and rapidly gives a stationary response, whereas the desorption time can be strongly reduced when a positive voltage pulse is applied to the gate for a short time (a few minutes).

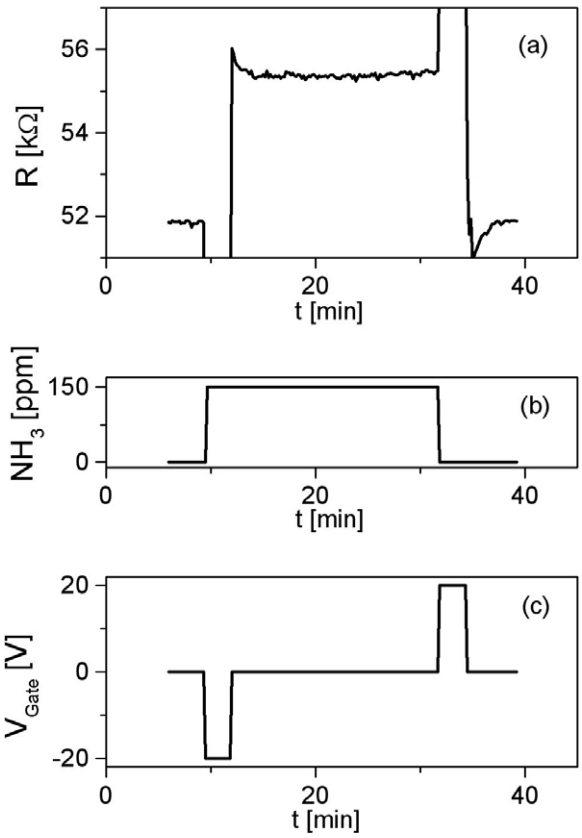

Figure 7. Timescale of the sensor response under the effect of negative and positive gate voltage: (a) resistance changes due to adsorption–desorption processes; (b) gas flow; (c) gate voltages. NH_3 concentration: 150 ppm.

The effects of the electrostatic perturbation on the kinetics of gas adsorption/desorption have been further investigated under transient conditions, as experienced in other works [33, 34].

In order to check that no memory effects are acting when a gate voltage is applied, and to verify that the response is dependent only on gas exposure, we performed different experiments.

First we checked, using pure nitrogen, that on applying a positive bias there is no response after the transient ($\Delta R/R \approx 0$). The same result was confirmed on applying a negative bias.

The second step was carried out in the presence of a fixed amount of ammonia (75 ppm). Figure 8 shows that by applying a variable number (five and eight) of negative pulses (-20 V, each one 1 min) the signal, after the transient, reaches every time the same $\Delta R/R$ value; i.e., with the same concentration we obtain the same response although a different gate pulse is applied. The adsorption steps are followed by two desorption steps, performed by applying four pulses of $+20$ V. From figure 8 one observes that at the end of each desorption step the base line of the relative resistance is precisely reproduced.

In figure 9 are reported the signals obtained from the third experiment, when the sensor was exposed to three different ammonia concentrations (75 ppm, 150 ppm, 300 ppm). In this experiment we applied during the absorption step the same number of pulses, namely five pulses of -20 V (each one 1 min). As one can see in figure 9, for the three different NH_3

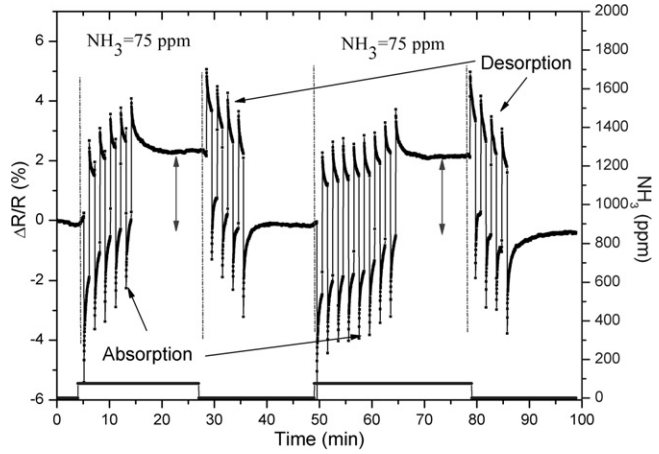

Figure 8. Sensor response under applied gate pulses in the presence of the same ammonia concentration (75 ppm). Adsorption step, variable number of −20 V pulses; desorption step, four pulses of +20 V.

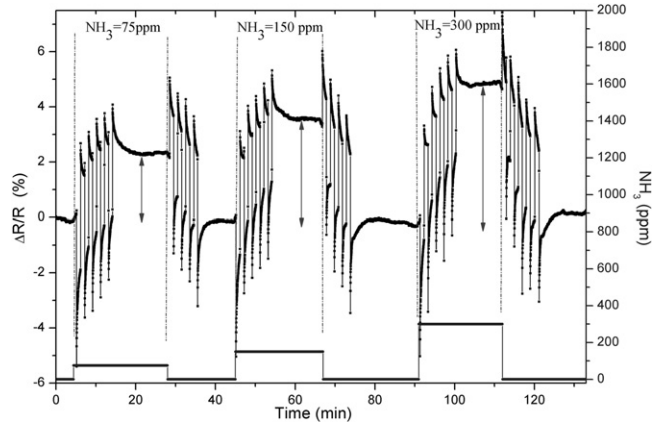

Figure 9. Sensor response under applied gate pulses for three ammonia concentrations (75 ppm, 150 ppm, 300 ppm). Adsorption step, five pulses of −20 V; desorption step, variable number of +20 V pulses.

concentrations, three different $\Delta R/R$ values, proportional to the concentrations, have been detected after the transient.

In figure 9 is also reported, for each ammonia concentration, the desorption process (+20 V, pulses of 1 min). Under the action of the positive pulses, very short times (less than 10 min) are needed to refresh the sensor after each measurement. The findings of these experiments clearly indicate that the response of the sensor depends exclusively on gas exposure and not on memory effects induced by the bias.

The conductance modulation after the application of the gate pulses and the resulting enormous acceleration of either the absorption time and the restoration time of the sensor can be rationalized on the basis of the following considerations.

A negative bias applied to the gate during the exposure of the sensor to the NH_3 molecules accelerates the absorption of ammonia, since NH_3 is characterized by an electron-

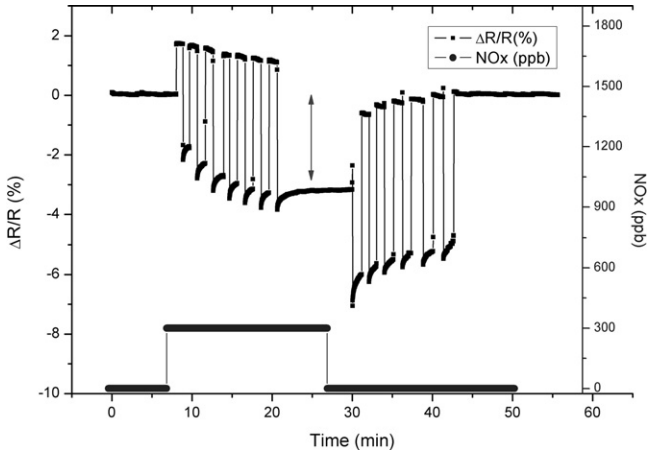

Figure 10. Sensor response under applied gate pulses in presence of 300 ppb of NO_x. Adsorption step, seven pulses of +20 V; desorption step, six pulses of −20 V.

donor behaviour. The negative gate polarizes positively the SWNT active layer inducing an electrostatic attraction between the gas molecules and the nanotube walls. The resulting effect is an improvement of the absorption rate. When a positive bias is applied to the gate during the desorption phase, the kinetics of the molecular interaction between NH_3 and SWNTs experiences an abrupt acceleration. The ammonia molecules are forced to desorb and are driven away by the local potential at the surface of the sensor.

For the electron acceptor NO_x an inverse behaviour has been evidenced with respect to NH_3. In figure 10 are reported the results of an experiment performed using 300 ppb of NO_x and applying +20 V pulses (7 pulses of 1 min) during the absorption phase and −20 V pulses during the desorption phase.

Also in the presence of the NO_x species the conductance changes occurred on a very fast timescale (less than 15 min) and were perfectly reversible.

Overall, the improvement of sensor response time with both NO_x and NH_3, obtained applying an electrostatic perturbation, can be justified by the polar nature of these molecules and their different bias polarities due to their different electronic properties (electron donor/acceptor).

4. Conclusions

Deposits formed by arrays of SWNT bundles have been used for the assembly of highly sensitive gas detectors operating at room temperature. A specific study has been dedicated to the purification of nanotube material and to nanotube manipulation. For the preparation of the sensing material both electrophoresis and dielectrophoresis processes were preliminarily tested using SWNTs dispersed in various solvents. The fabrication of the sensor was performed by drop depositing dispersions of SWNTs in $CHCl_3$ onto the interdigitated area of an electrode platform and applying AC fields (10 V_{pp}, 1 MHz).

The effects of different voltages (+20 V, 0 V, −20 V) applied to the back gate of the devices exposed to different concentrations of NO_x and NH_3 have also been analysed. On the basis of the present results it can be concluded that among the different parameters [30, 33, 34] that can affect the performances of gas sensors based on SWNTs the biasing of the gate contact

is one of the most effective and that an appropriate voltage can be used to increase the overall sensitivity. From the experiments the detection limits are estimated as a few ppb for NO_x and a few ppm for NH_3, respectively. Moreover, we evidenced a dramatic improvement in the time dependent behaviour of the device by properly tuning the gate voltage.

For NH_3 a transient negative voltage was found to facilitate the absorption process and reaching the steady condition of the device after gas exposure. Conversely, a positive gate voltage pulse helps to reset the status of the device, accelerating the desorption time by two orders of magnitude.

Similar results are obtained for the acceleration of the sensor response to NO_x detection. However, the sign of the gate voltage is in this case opposite with respect to the case of ammonia.

The present analysis indicates that the detection of a few ppm NH_3 or a few ppb NO_x is achieved in some hundreds of microseconds and that after 1 min the sensor is ready for a new operation.

When dealing with different chemical species it is necessary to identify the mechanism of their interaction with the SWNTs and to select a specific sequence of positive/negative back-gate voltages that could accelerate the time response of the sensor. The capability of tuning the interaction of gas molecules with the nanotubes by a proper sequence of negative and positive biasing may result in a significant improvement of the sensing performances of such devices that can be used for controlling industrial processes as well as for monitoring domestic and environmental safety.

Acknowledgments

This work has been performed in the frame of the project MIUR-PRIN 2004, and of the FIRB National Program.

References

[1] Han H, Vijayalakshmi S, Lan A, Iqbal Z, Grebel H, Lalanne E and Johnson A M 2003 *Appl. Phys. Lett.* **82** 1458
[2] Xiao K, Liu Y, Hu P, Yu G, Wang X and Zhu D 2003 *Appl. Phys. Lett.* **83** 150
[3] Lucci M, Regoliosi P, Reale A, Di Carlo A, Orlanducci S, Tamburri E, Terranova M L, Di Natale C, D'Amico A and Paolesse R 2005 *Sensors Actuators* B **111/112** 181–6
[4] Iijima S 1991 *Nature* **354** 56
[5] Gulseren O, Yildirim T and Ciraci S 2003 *Phys. Rev.* B **68** 115419
[6] Kleinhammes A, Mao S H, Yang X J, Tang X P, Shimoda H, Lu J P, Zhou O and Wu Y 2003 *Phys. Rev.* B **68** 075418
[7] Lantz M A, Gotsmann B, Dürig U T, Vettiger P, Nakayama Y, Shimizu T and Tokumoto H 2003 *Appl. Phys. Lett.* **83** 1266
[8] Rotkin S V, Ruda H E and Shik A 2003 *Appl. Phys. Lett.* **83** 1623
[9] Chopra S, McGuire K, Gothard N, Rao A M and Pham A 2003 *Appl. Phys. Lett.* **83** 2280
[10] Peng S and Cho K 2000 *Nanotechnology* **11** 57
[11] Collins P G, Bradley K, Ishigami M and Zettl A 2000 *Science* **287** 1801
[12] Verghese O K *et al* 2001 *Sensors Actuators* **81** 32
[13] Kong J, Franklin N R, Zhou C, Chapline M G, Peng S, Cho K and Dai H 2000 *Science* **287** 622
[14] Li J, Lu Y, Cinke M, Han J and Meyyappan M 2003 *Nano Lett.* **3** 929
[15] Modi A, Koratkar N, Lass E, Wei B and Ajayan P M 2003 *Nature* **424** 171
[16] Saito Y, Nishiyama T, Kato T, Kondo S, Tanaka T, Yotani J and Uemura S 2002 *Mol. Cryst. Liq. Cryst.* **387** 303
[17] Cinke M, Li J, Chen B, Cassell A, Delzeit L, Han J and Meyyappan M 2002 *Chem. Phys. Lett.* **365** 69
[18] Adu C K W, Sumanasekera G U, Pradhan B K, Romero H E and Eklund P C 2001 *Chem. Phys. Lett.* **337** 31
[19] Terranova M L, Orlanducci S, Fazi E, Sessa V, Piccirillo S, Rossi M and Manno D 2003 *Chem. Phys. Lett.* **381** 86

[20] Smith B W, Benes Z, Luzzi D E, Fischer J E, Walters D A, Casavant M J, Schmidt J and Smalley R M 2000 *Appl. Phys. Lett.* **77** 663
[21] Kim Y C, Sohn K H, Cho Y M and Yoo E H 2004 *Appl. Phys. Lett.* **84** 5350
[22] Chung J, Lee K-H, Lee J and Ruoff R S 2004 *Langmuir* **20** 3011
[23] Chen X Q, Saito T, Yamada H and Matsushige K 2001 *Appl. Phys. Lett.* **78** 3714
[24] Krupke R, Hennrich F, Löhneysen H V and Kappes M 2003 *Science* **301** 344
[25] Chen X Q, Saito T, Yamada H and Matsushige K 2004 *Appl. Phys. Lett.* **84** 3714
[26] Yamamoto K, Akita S and Nakayama Y 1998 *J. Phys. D: Appl. Phys.* **31** L34
[27] Chan R H M, Fung C K M and Li W J 2004 *Nanotechnology* **15** S672–7
[28] Krupke R, Hennrich F, Weber H B, Beckmann D, Hampe O, Malik S, Kappes M M and Lohneysen H V 2003 *Appl. Phys.* A **76** 397–400
[29] Valentini F, Amine A, Orlanducci S, Terranova M L and Palleschi G 2003 *Anal. Chem.* **75** 5413–21
[30] Lucci M, Reale A, Di Carlo A, Orlanducci S, Tamburri E, Terranova M L, Davoli I, Di Natale C, Paolesse R and D'Amico A 2006 *Sensors Actuators* B **118** 226–31
[31] Buldum Z A, Han J and Lu J P 2002 *Nanotechnology* **13** 195–200
[32] Tompkins F C 1978 *Chemisorbtion of Gases on Metals* (New York: Academic Press)
[33] Novak J P, Snow E S, Houser E J, Park D, Stepnowski J L and McGill R A 2003 *Appl. Phys. Lett.* **83** 4026–8
[34] Snow E S, Novak J P, Campbell P M and Park D 2003 *Appl. Phys. Lett.* **82** 2145